REPORT DOCUMENTATION PAGE

Form Approved OMB No. 0704-0188

1. REPORT DATE *(DD-MM-YYYY)*	2. REPORT TYPE	3. DATES COVERED *(From – To)*
25-02-2008	Final Report	25 September 2004 - 25-Sep-06

4. TITLE AND SUBTITLE

Steps towards Large Scale Production of High-Spin Hafnium Isomers by Spallation Reactions

5a. CONTRACT NUMBER
FA8655-04-1-3046

5b. GRANT NUMBER

5c. PROGRAM ELEMENT NUMBER

6. AUTHOR(S)

Dr. Calin Ur

5d. PROJECT NUMBER

5d. TASK NUMBER

5e. WORK UNIT NUMBER

7. PERFORMING ORGANIZATION NAME(S) AND ADDRESS(ES)

Induced Gamma Emission Foundation
PO Box 34-81
Bucharest 024280
Romania

8. PERFORMING ORGANIZATION REPORT NUMBER

N/A

9. SPONSORING/MONITORING AGENCY NAME(S) AND ADDRESS(ES)

EOARD
Unit 4515 BOX 14
APO AE 09421

10. SPONSOR/MONITOR'S ACRONYM(S)

11. SPONSOR/MONITOR'S REPORT NUMBER(S)
Grant 04-3046

12. DISTRIBUTION/AVAILABILITY STATEMENT

Approved for public release; distribution is unlimited.

13. SUPPLEMENTARY NOTES

14. ABSTRACT

This report results from a contract tasking Induced Gamma Emission Foundation as follows: The contractor will investigate the production and accumulation of the nuclear isomer 178m2 Hafnium by spallation of hafnium targets with high-energy protons. The Hafnium yield will be assayed and compared to predictions. The program will use Hf targets for the optimization of the 178m2Hf yield and for the minimization of the running cost related to the simplicity and availability of accelerators operating at such low energies.The operation cost for a small cyclotron that provides protons of energies around 150 MeV are order of magnitude lower than those for the operation of the Los Alamos 800 MeV meson factory facility. By the end of the first year the Foundation will have the results of the data analysis for the irradiation of the natural Hf targets and LAHET calculations will be recalibrated based on the new experimental data. The technical problems related to the design and mounting of Hf targets including heat removal solutions will be settled. Working from this base the Foundation will contract the irradiation of the enriched Hf targets at the Dubna synchrocyclotron establishing all the details concerning the beam energies, number of the irradiations and their duration.

15. SUBJECT TERMS
EOARD, Gamma ray emission, Isomer production, Numerical Simulation

16. SECURITY CLASSIFICATION OF:			17. LIMITATION OF ABSTRACT	18, NUMBER OF PAGES	19a. NAME OF RESPONSIBLE PERSON
a. REPORT	b. ABSTRACT	c. THIS PAGE			A. GAVRIELIDES
UNCLAS	UNCLAS	UNCLAS	UL	28	19b. TELEPHONE NUMBER *(Include area code)* +44 (0)1895 616205

Steps towards Large Scale Production of High–Spin Hafnium Isomers by Spallation Reactions

Final Report
EOARD GRANT NO: FA8655-04-1-3046-P00002

1. Introduction

The study of spallation reactions induced by high energy protons on heavy targets experience a renewed interest nowadays as many advanced applications are based on their use. The applications using spallation reactions can be divided in two categories. One is related to the production of intense neutron beams through the bombardment a thick heavy target with intense high energy proton beams of interest for material science physics research or accelerator–driven systems for nuclear waste transmutation and subcritical reactors; there are two main projects using this technique under development at the present time: the European Spallation Source (ESS) [1] and the Spallation Neutron Source (SNS) at Oak Ridge [2]. The other category of application using spallation reactions is the production of exotic nuclei for nuclear physics research along with projectile fragmentation and fission techniques. There is currently an increased interest in developing beams of isomeric nuclei for the nuclear physics research [3, 4]. It was discussed [3] that by using high–spin isomeric nuclei as secondary beams in fusion reactions one can produce compound nuclei at higher angular momentum due to the contribution of the intrinsic spin of the isomers while competition with fusion–fission processes at similar high spin values is less restrictive than in the case of the fusion reactions with stable nuclei. One of the main issues related to the production of isomeric beams is their purification. Evidently, traditional mass separators cannot discriminate isomeric nuclei from their ground state. Recent technical developments provided new solutions that are already in use or they will be shortly available. Laser resonance ionization, based on the energy differences of the atomic levels due to the hyperfine interaction of the electrons with the different nuclear spins of the ground state and the isomeric state, was successfully used at ISOLDE on–line isotope separator and it was shown for the case of ^{68g}Cu/^{68m}Cu that the isomeric–to–ground state ratio can be increased by a factor of about 400 [5, 6]. Laser resonance ionization is not always applicable; it is the case of the fragment separator FRS at GSI that can isotopically separate the secondary beams but cannot produce pure isomeric beams. It was shown in Ref. [7] that in this case a high resolution mass separation can be achieved by using cooled beams in a storage ring.

The research interest of the IGE Foundation focused on the use of spallation reactions as source of long–lived isomers. We investigated the production of high–spin isomers in the mass region A≈180 by using spallation of heavy targets with protons of intermediate energy. We devoted a particular attention to the production of the ^{178}Hf^{m2} isomer. This isomer is a singular case in the nuclear landscape; it is located at about 2.45 MeV excitation energy, it has spin and parity $J^{\pi}=16^{+}$ and a half–life of 31 years, and decays through gamma–ray emission. Since its discovery in 1968 [8] a lot of experimental work was devoted to understand its structure and decay properties. The isomer was assigned a four quasi–particle (2 proton–type

and 2 neutron–type) configuration [8, 9] being the band head of a high–K rotational structure [10, 11] with K = 16. The main decay (99.9%) goes through a highly converted 13 keV E3 gamma–ray transition to the 13^- state of the $K^\pi = 8^-_1$ band. A recent high sensibility measurement of the isomer decay [12] established precisely its location at 2446.0 keV excitation energy. The remarkable long lifetime of the isomer is the result of the combined effect of the K quantum number selection rules and location of the isomer at excitation energy lower than any other state with spin 14 ħ or higher, a characteristic of the yrast traps. It was discussed in [12] that K–mixing leads to a relaxation of the K selection rules and one has to speak about hindrance of the γ–ray transitions rather then forbiddenness. This effect was quantified in terms of the reduced hindrance or hindrance per degree of K forbiddenness, f_v. It is interesting that in the case of the ^{178m2}Hf isomer large reduced hindrance values were found (115±50) in contrast with the decay of other four quasi–particle isomers in neighboring nuclei (f_v=2 in ^{182}Os or f_v=5 in ^{174}Hf) [12]. Very recently [13] it was shown in Coulex measurements of ^{178}Hf that K–mixing develops in the low–K bands and increases with the spin value up to the complete breakdown of the K quantum number at spins higher than 12 ħ while the high–K bands remain quite pure.

The long lifetime of the ^{178m2}Hf isomer made it very attractive for the development of isomeric beams since long time [14]. The main difficulty is to produce pure isomeric beams under the conditions of very low isomeric–to–ground state ratio values from the production reactions. Recent advances in the use of cooled beams in storage rings [7] show that one can attain the levels of sensibility needed to separate ^{178m2}Hf isomers from the ^{178}Hf ground state nuclei ($\Delta M_{(m2-g)}/M_g = 1.5x10^{-5}$). An important advantage of the ^{178m2}Hf isomers over other high–spin isomers is the possibility to accumulate the isomeric nuclei for long time and produce isomeric targets that can be stored for long time before use.

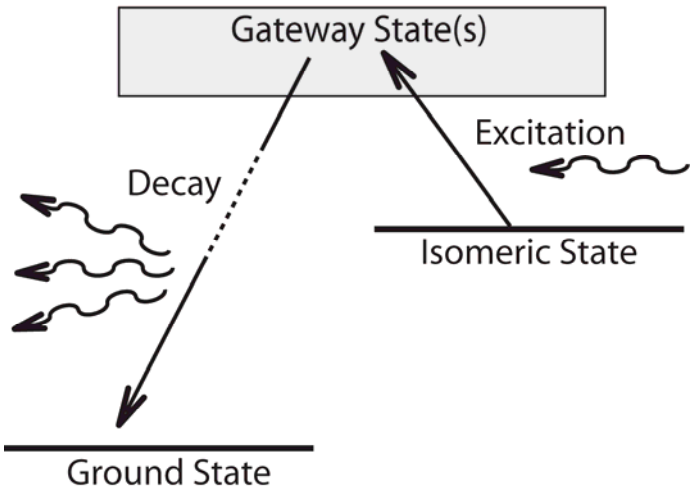

Fig. 1 – Illustration of the two–step induced decay of an isomeric state when exposed to external radiation field.

Important applications as the development of γ–ray lasers (see Ref. [15] and references therein) are related to the possibility of triggering the release of the energy stored in isomeric states under the action of external radiation fields. The scenario of a two–step process is illustrated in Fig. 1: isomeric nuclei absorb the external radiation and are excited to gateway state(s); the structure of the gateway states is such that their decay–out is not anymore forbidden or hindered; after emission of a cascade of fast γ–rays bypassing the isomeric state nuclei reach their ground state.

Such an effect was observed for the first time by a distinguished member of the IGE Foundation in ^{180}Ta [16]. The ground state of ^{180}Ta has $J^{\pi} = K^{\pi} = 1^{+}$ and a half–life of 8.15 h while the isomeric state $J^{\pi} = K^{\pi} = 9^{-}$ located at 77.1 keV excitation energy [17] has a lifetime of $>1.2 \times 10^{15}$ years. Following the exposure of samples containing such long–lived isomers to an intense Bremsstrahlung radiation from a 6 MeV medical linac the characteristic X–rays of the ground state decay daughters (^{180}Hf–86% EC and ^{180}W–14% β^{-}) were detected. The result was later confirmed by several other measurements (see Refs. [18, 19] for example) and it was established that the minimum energy needed for inducing the decay of the isomer is about 1 MeV. While it is generally accepted that the observed integrated cross–section for the photon–induced decay of the 9^{-} isomeric state in ^{180}Ta does not contradict the standard nuclear physics recommended upper limits and sum–rules, the experimental data are by more than 2–3 orders of magnitude higher than state–of–the–art nuclear model calculations can predict [19]. The case of ^{180}Ta is of no practical interest given the largely unfavorable ratio between the energy needed to trigger the isomer decay and the net energy gain of the process; its importance was the first demonstration of the possibility to trigger emission of γ rays from isomeric nuclei. A way more attractive case is the *m2* isomeric state of ^{178}Hf because of its high excitation energy and long lifetime. It was assumed that in this case a similar triggering process can be also induced but with a much lower energy electromagnetic radiation. Measurements performed with a dental X–ray source (Ref. [20] and references therein) and at Spring8 synchrotron [21] brought evidence in favor of such a process ignited by X–rays of energy as low as ~10 keV.

The recently reported Coulomb excitation experiments [13] affirm that no states that might mediate the above discussed induced γ–ray emission were found. This is not surprising given the very different nature of the photo–excitation and Coulomb excitation processes (in Coulomb excitation E2 and E3 transitions are preponderantly favored) and does not necessarily mean that such states do not exist.

The studies with ^{178m2}Hf are strongly limited by the very low inventory of such isomers available around the world. A synthetic summary of the ^{178m2}Hf isomers production schemes is presented in Ref. [22]. The main production methods investigated until now are:

i) <u>*Fusion–evaporation reactions*</u>. The ^{176}Yb(α,2n)^{178m2}Hf reaction was used at JINR Dubna [23]. The maximum cross–section for the formation of the isomer is about 9 mb and the isomer–to–ground state (σ_m/σ_g) ratio is about 5%. The number of byproducts is reduced. The method requires a large accelerator to produce the α beam.

ii) <u>*Neutron induced reactions*</u>. The reactions with thermal and low–energy neutrons as ^{177}Hf(n,γ) and ^{178}Hf(n,n' γ) have very low cross–sections of the order of 10^{-2}–10^{-3} mb with σ_m/σ_g ratio of the order of 10^{-9}–10^{-6} [24]. They require the use of a nuclear reactor for the

irradiations and result in a large number of byproducts. The reaction ^{179}Hf(n,2n) with protons of 14.5 MeV has a cross section of about 7 mb that is at the level of the fusion–evaporation reactions and with $\sigma_m/\sigma_{g\ ratio}$ only one order of magnitude lower [25]. The number of byproducts is relatively small. With the latest development of compact neutron sources able to deliver relatively high neutron fluxes at 14 MeV [26] this method might be revisited in the future.

iii) *Spallation reactions*. The process that produced the largest quantity of ^{178m2}Hf isomers (10^{17}) until now was the spallation with a 400 μA proton beam at 800 MeV energy of a ~1 kg Ta beam dump at the Los Alamos National Laboratory LAMPF meson factory [27]. The resulting σ_m/σ_g ratio is intermediate between the values for the fusion–evaporation and the (n,2n) reactions. The main disadvantages of this method are the use of a huge accelerator to produce the high–energy proton beam and the extremely high activity of the irradiated samples due to the relatively long–lived byproduct radionuclei.

We account in this report on the production of ^{178m2}Hf isomers through spallation of enriched ^{179}Hf targets with intermediate energy protons. A brief overview of the previous spallation measurements performed by the IGE Foundation is also presented. The main interest was focused on the production of ^{178m2}Hf but also other high–spin isomers as ^{177m}Lu (E_x = 970.2 keV, J = 23/2 ħ, $T_{1/2}$ = 160.4 d) or ^{179m2}Hf (E_x = 1105.8 keV, J = 25/2 ħ, $T_{1/2}$ = 25.1 d) could be identified and measured.

2. General remarks on the spallation process

The use of spallation reactions to produce high–spin isomers as ^{178m2}Hf has to face several problems concerning the reaction mechanism and the characteristics of the isomer. Spallation reactions populate mainly neutron–deficient nuclei that in turn decay through EC and β^+ processes towards stable isobars. The ^{178}Hf nucleus is located on the β–stability line and its direct or independent population from spallation has a low cross–section; it results mainly in the ground state as cumulative decay of higher Z isobars. On the other hand, the ^{178m2}Hf isomer, due to its high excitation energy and spin, can result exclusively from independent population. The total cross–section of the ^{178}Hf independent population is spread over many states of lower spin and excitation energy leading to a reduction of the cross–section for the isomer production.

Practically, the independent–to–cumulative ratio for ^{178}Hf and the isomer–to–ground state ratio define the obtained yield of ^{178m2}Hf. Both ratios are difficult to predict by calculations and our experimental results bring valuable information for the calibration of the computer code simulations.

The use of high energy proton beams will obviously favor direct population of states with high excitation energy but at the same time it will move the mass distribution of the spallation products towards emission of a larger number of nucleons. It is clear that production of the high–spin isomer ^{178m2}Hf is subjected to a very delicate balance between the target material and the proton beam energy. Low incident energies will favor production of nuclei in the vicinity of the target while high energies will move the peak of the mass

distribution away from the target mass. Spallation at moderate and high proton energies favor population of nuclei emitting many neutrons and only few protons meaning that the target material has to be only few protons away from Hafnium but as rich as possible in neutrons. Fig. 2 illustrates these concepts in a simple and intuitive picture.

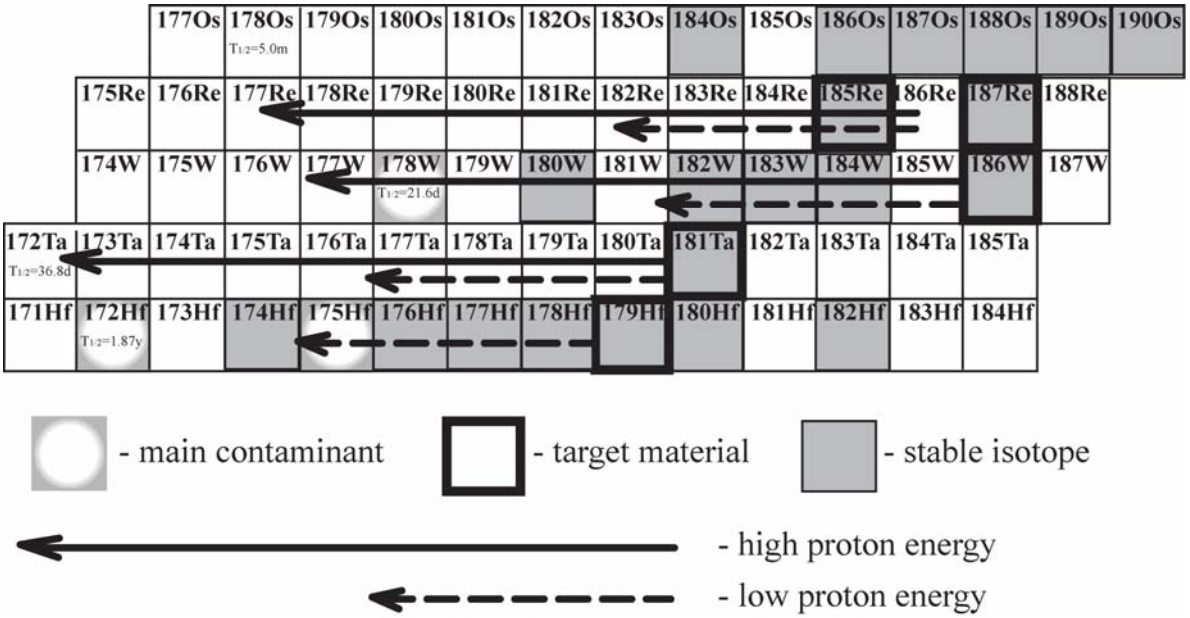

Fig. 2 – Schematic illustration of the extension of the populated nuclei through spallation processes induced by low and high energy protons on different heavy targets. The arrows show the mass regions populated by using low and high energy protons.

To characterize the different combinations of proton beam energy and target material we identified some quality indicators:

- the absolute yield of the ^{178m2}Hf isomer;
- the isomer–to–ground state ratio;
- the yield of the long–lived contaminants;
- the cooling time of the samples.

One has to find the optimal combination of these parameters to identify the best reaction for the isomer production.

When we started this work, almost one decade ago, we realized that the experimental cross–section measurements through reactions induced by protons with energy in the range of 0.1–1.0 GeV were not yet well known. Data were fragmentary, as reported in Ref. [28], and many of the known values were measured mostly in the period 1960–1970 with limited accuracy.

We performed a systematic study of proton–induced spallation reactions at intermediate beam energies on several heavy targets: ^{nat}Ta, ^{nat}Re[29], ^{nat}W and ^{186}W [30], and ^{nat}Hf under the following EOARD grants: F61775–99–WE030, F61775–00–WE056, FA8655–02–1–3069 and FA8655–04–1–3046.

3. Previous measurements

3.1. The p + ^{nat}Ta reaction

We started with the study of the p + ^{nat}Ta reaction for historical reasons. This was the reaction that produced the largest quantity of ^{178m2}Hf isomer (10^{17}) until now. Production of ^{178m2}Hf isomer in this case resulted as a byproduct of the operation of the LAMPF accelerator [27] and was never optimized for this purpose. The irradiation of a massive beam dump of ^{nat}Ta with a 400 μA proton beam at 800 MeV produced highly radioactive samples that were left to cool down for a long period of time before they could be safely handled. Many Hf isotopes were produced in this reaction with yields orders of magnitude larger than ^{178m2}Hf; two of them ^{175}Hf ($T_{1/2}$ = 70 d) and ^{172}Hf ($T_{1/2}$ = 1.87 y) produced an intense γ radiation background for more than a decade so that the chemically separated Hf fraction could be used only 20 years after the irradiation.

Three ^{nat}Ta targets with a thickness of 33.3 g/cm^2 (about 2 cm thick along the beam direction) were irradiated with protons of 660, 200 and 100 MeV, respectively, at internal locations of the accelerator. A fourth irradiation was performed using the extracted 660 MeV proton beam and a target consisting of a stack of two thin foils of Ta (156 mg/cm^2) and Al (30.6 mg/cm^2). This way the two foils were exposed to the same beam fluence. The cross–sections for the production of ^{7}Be and ^{22}Na through the p + Al reaction were measured with high accuracy in Ref. [31] and they were used to calibrate the cross–section of the products. Natural Ta contains 99.988% of ^{181}Ta and 0.012% of the long–lived isomer ^{180m}Ta (>1.2 x 10^{15} years) so that we could safely consider the samples as being mono–isotopic (^{181}Ta) for all the considerations. The yield of the radionuclide ^{178}W produced in the reaction ^{181}Ta(p, 4n)^{178}W is known with high accuracy [32] and, since the γ rays associated with its decay are strong, it could also be used for cross–section and γ–ray energy calibration purposes.

3.2. The p + ^{nat}Re reaction

In the case of the ^{nat}Re irradiation, the targets were of 21 g/cm^2 thickness (about 1 cm thick). Four targets were exposed to the internal beam at different incident energies, 150, 300, 450 and 660 MeV, respectively. As in the case of Ta irradiation, a stack of two foils of ^{nat}Re and Al of comparable thickness (0.56 mg/cm^2) were irradiated with the 660 MeV extracted beam for cross–section calibration purposes. After irradiation, the targets were left for 3 weeks to cool down before the first activity measurement was performed. As a result radionuclides with half–lives shorter than 2 days could not be detected. The weakest activity determined with our method corresponds to a production cross–section as low as 1 μb. The ^{nat}Re contains two components, ^{185}Re and ^{187}Re with abundancies of 37.4% and 62.6%, respectively. Intense γ rays corresponding to ^{185}Os and ^{183}Re were identified in the measured spectra; they are populated through the ^{187}Re(p, 3n)^{185}Os and ^{187}Re(p, p4n)^{183}Re reactions. Similar reactions with ^{181}Ta target were accurately measured [32].

3.3. The p + ^{nat}W and p + ^{186}W reactions

The ^{178}Hf nucleus is located near the beta stability line and the cross section for its population through spallation is low; the use of target nuclei as reach as possible in neutrons will populate better such nuclei. Spallation at moderate and high proton energies favor population of nuclei emitting many neutrons and only few protons meaning that the target material has to be only few protons away from Hafnium but as rich as possible in neutrons. A survey of the available isotopes in the neighborhood of ^{178}Hf indicated ^{186}W as the best target candidate. Its natural abundance is 28.6% and we used enriched material at the level of 96.8% in order to eliminate the contribution from the other lighter W isotopes to the final results.

Three targets of enriched ^{186}W (96.8%) in metallic form were built. Each target was about 7 mm thick. The ^{186}W targets were placed on a 50 μm ^{nat}W backing and, then fixed on the cooled Al holder. The irradiations of the samples were performed at the internal beam of the synchrocyclotron. The position of the targets inside the accelerator was chosen to provide incident beam energies of 650, 450 and 300 MeV, respectively. The particular design of the targets allowed for the simultaneous irradiation of the enriched ^{186}W material and of the ^{nat}W holder foil under identical conditions allowing for a direct comparison of the results for both materials. After irradiation the samples were cooled for 1 month so that short–lived radionuclides could not be measured by our method.

3.4. The p + ^{nat}Hf reactions

The first part of the present Grant was used for an exploration run meant to understand whether the use of Hf as target material can be considered for the production of ^{178m2}Hf isomer. The irradiation of ^{nat}Re targets [29] resulted in a significant yield of the ^{184m}Re isomer at low proton energy around 100 MeV. Since the natural composition of Re is : ^{185}Re – 37.4% and ^{187}Re – 62.6%, the only ways to populate the isomer are the reactions: ^{185}Re(p,p′n)^{184m}Re and ^{187}Re(p,p′3n)^{184m}Re with no net loss of protons. Such processes are opposite to the ‘evident’ direction we tried before when population of the ^{178m2}Hf was reached through spallation processes ignited by high energy protons and where many nucleons are emitted. This observation opened new perspectives on the production of the ^{178m2}Hf high–spin isomer with relatively low energy protons. The use of low energy protons has several advantages as reduced yield of the main contaminants with a resulting shorter cooling time of the irradiated samples, a larger availability of accelerators delivering such energies, lower operation costs for the smaller accelerators. Of course, there is also a drawback of using the Hf as target material, that is, the impossibility to chemically separate the isomers from the bulk material. For these reasons we considered important to have such an investigative run to explore the potentiality of the natural Hf material for producing the ^{178m2}Hf isomer before using enriched Hf targets.

Four targets of 13.3 g/cm^2 thickness (1 cm thick) were irradiated with protons at 650, 450, 250 and 120 MeV. The activity of the targets immediately after irradiation was rather high due to the use of massive targets and high beam intensities and, hence, cooling of the targets for one month was necessary before performing γ–ray activity measurements. Afterwards, the targets were left to cool down for another two and a half months. Since the background γ–ray activity was still too high to allow identification of the weak activity associated with the decay of the ^{178m2}Hf isomer we performed the chemical purification of the material from other elemental compounds. The chemical procedure was modified to account for the fact that in this case the bulk material was Hf itself. The isotopic composition of ^{nat}Hf is: ^{180}Hf–35.08(16)%, ^{179}Hf–13.62(2)%, ^{178}Hf–27.28(7)%, ^{177}Hf–18.60(9)%, ^{176}Hf–5.26(7)%, ^{174}Hf–0.16(1)%. Therefore, when using a ^{nat}Hf target, the ^{179m2}Hf and ^{178m2}Hf isomers can be produced exclusively through the following reactions: ^{180}Hf(p,p′n)^{179m2}Hf, ^{180}Hf(p,p′2n)^{178m2}Hf and ^{179}Hf(p,p′n) ^{178m2}Hf and inelastic scattering of protons.

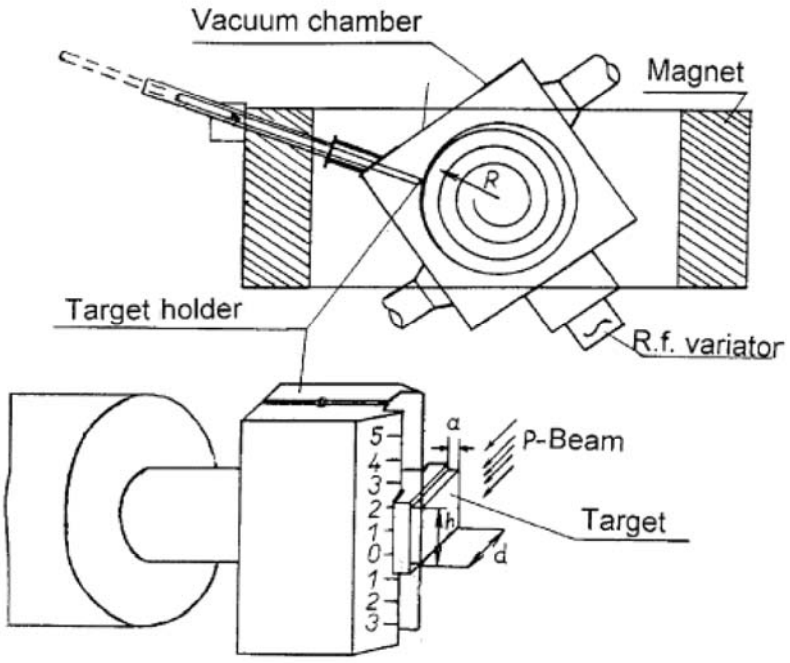

Fig. 3 – The 6m synchrocyclotron (phasotron) of LNP, JINR Dubna. Targets can be irradiated at different energies by inserting them at different radii inside the accelerator. The inset shows an enlarged image of the target holder. The target is placed tangent to the direction of the beam so that even thin targets present a large effective thickness along the beam direction. In the cyclotron the protons follow almost circular orbits. Different radii correspond to different proton energies, e.g. a 120 cm radius correspond to 110 MeV proton energy.

Based on a qualitative discussion [33] and taking into account the spin–deficit parameter (the difference between the final spin of the isomer and the total initial spin of the system) we concluded that ^{178m2}Hf is mainly produced in the ^{179}Hf (p,p′n) reaction and its relatively low yield in the (p + ^{nat}Hf) irradiation is related to the low abundance of ^{179}Hf –

13.62(2)% – in the natural composition samples. For ^{179m2}Hf we concluded that it should be the same process ^{180}Hf(p, p′n) that produce it. Since these reactions have similar spin deficit, the isomer yields ratio ^{179m2}Hf/^{178m2}Hf has to be determined primarily by the isotopic abundance ratio ^{180}Hf/^{179}Hf in the natural composition Hafnium samples (about 0.39). The experimentally measured value of the ratio ^{179m2}Hf /^{178m2}Hf was 0.44 very close to what we expected to get from our qualitative discussion. In the case of enriched ^{179}Hf samples, where the ratio of the isotopes ^{180}Hf/^{179}Hf favors the ^{179}Hf(p,p′n)^{178m2}Hf process we expected a large increase of the ^{178m2}Hf isomer yield. Consequently, we decided to perform irradiations of enriched ^{179}Hf samples with low energy protons and compare the results with the ones obtained from the irradiation of natural Hf.

4. Irradiation of the enriched ^{179}Hf

4.1. The experimental setup

The irradiations were performed at the Laboratory of Nuclear Problems of the Joint Institute for Nuclear Research Dubna. The proton beam was delivered by the 6m Synchrocyclotron (phasotron).

The maximum proton energy reachable with this accelerator is 660 MeV; irradiations at lower energies can be performed with the internal beam at different radial positions. The proton beam intensity was about 2–3 μA. There is no precise way to measure the beam intensity at the internal beam positions and for this reason we will not use this rough value for the evaluation of the cross–sections but we will rather calibrate the fluence of the beam with the known cross–section values in the Hf and Al backing.

The targets and their holder were optimized for the efficient removal of the heat released by the beam in the targets. . The effective target thickness is defined by its size along the beam direction, as they are mounted tangent to the proton orbits. In this way, even thin foils result in ‘thick’ targets as the protons transit the whole width of the targets. A schematic representation of the experimental setup for the samples irradiations is shown in Fig. 3.

4.2. Target preparation

A high enrichment degree in ^{179}Hf combined with the results from the irradiation of natural Hafnium (essential to remove background contribution generated by the remaining Hf isotopes) provide the compulsory basis for a realistic quantitative estimate of the ^{178m2}Hf isomers production by the spallation of the ^{179}Hf samples. The highest degree of enrichment obtainable on the isotope market for ^{179}Hf was around 90%. The enriched material was available in the form of HfO_2 oxide powder. The composition of the enriched material used for the irradiations is given in Table 1. In all our previous irradiations (including the ^{nat}Hf irradiation) the targets were in metallic form. The reduction of the oxide to metallic form

results in large losses of material. So, for the case of the enriched ^{179}Hf samples in oxide form we had to develop a new target production procedure. Before producing the final targets with the enriched material we made tests with $^{nat}HfO_2$ powder. First, we tried to prepare layers of Hf oxide by mechanically pressing the powder on the Al backing. Poor quality samples were obtained this way. To solve the problem we used a chemical deposition. The Hf oxide was transformed into nitrate salt; the Hf nitrate was mixed with acetone and organic additives and the resulting paste distended onto a 10 μm thick Al foil. The foil was then heated up, the organic additives were burned out and the hydrated salt was reduced back to HfO_2 attached to the Al surface as a mechanically strong layer. The process of deposition was repeated many times up to reaching a 6–7 mg/cm^2 thickness mechanically strong layers of Hf oxide. Thicker layers are not as stable and are at risk of material loss during the irradiation.

Table 1. Composition of the Hafnium enriched in the ^{179}Hf isotope used to prepare the targets for the irradiations performed at the Dubna synchrocyclotron.

Isotope	174	176	177	178	**179**	180
Enrichment (%)	0.01	0.11	0.47	1.20	**90.7±0.3**	7.52

Once the procedure was thoroughly tested with natural Hf, we applied it for the preparation of enriched ^{179}Hf targets. The samples were prepared in the form of multiple folded sandwiches of $^{179}HfO_2$ layers deposited on Al foils. The dimensions of the layers were 10x15 mm. The target design is schematically shown in Fig. 3.

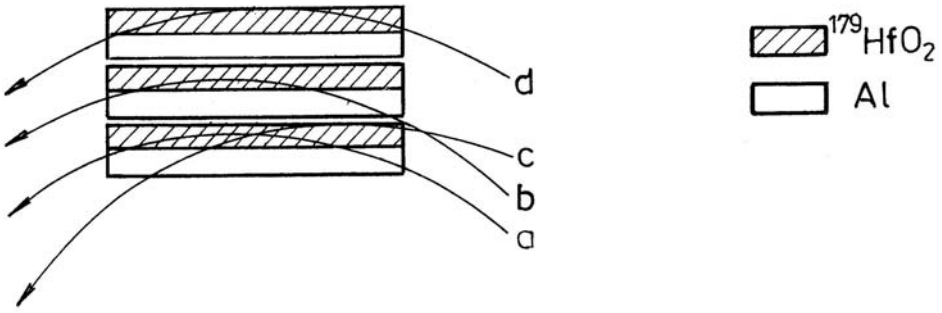

Fig. 4 – Schematic representation of a sandwiched–type $^{179}HfO_2$ sample; several composite $^{179}HfO_2$ layers attached to Al foils are fixed together and exposed to the proton beam. Possible proton trajectories through the sample are also represented.

Four such sandwiched–type targets, each containing about 70 mg of enriched ^{179}Hf were prepared. A similar sandwiched–type target of natural Hafnium oxide was prepared. The targets were fixed on the Al target holder in such a way to ensure the best thermal contact and removal of thermal load.

4.3. Irradiations and activity measurements

The targets are placed tangent to the proton trajectories and, since the curvature of the trajectories is low, the protons transverse the targets almost parallel to their surface. Examples of different trajectories of the protons across the targets are shown in Fig. 4. The range of the protons at the energies used for the irradiations is much longer than the thickness of the target (10 mm). As the protons travel through the target they interact with the matter and lose energy. One has to take into account all the different trajectories for calculating the mean energy loss of protons in the target. The trajectories preponderantly transverse both the HfO_2 targets and the Al holders; consequently, it is realistic to assume that the protons travel half of the path in HfO_2 and half in Al. The beam has also a vertical spread but it is within the width of the target (15 mm).

The first irradiation was performed with the natural Hafnium target at 300 MeV proton beam energy with the goal of testing the robustness of the target in the present construction and the ability of the mechanical mounting to efficiently removing the thermal load and avoid melting of the target.

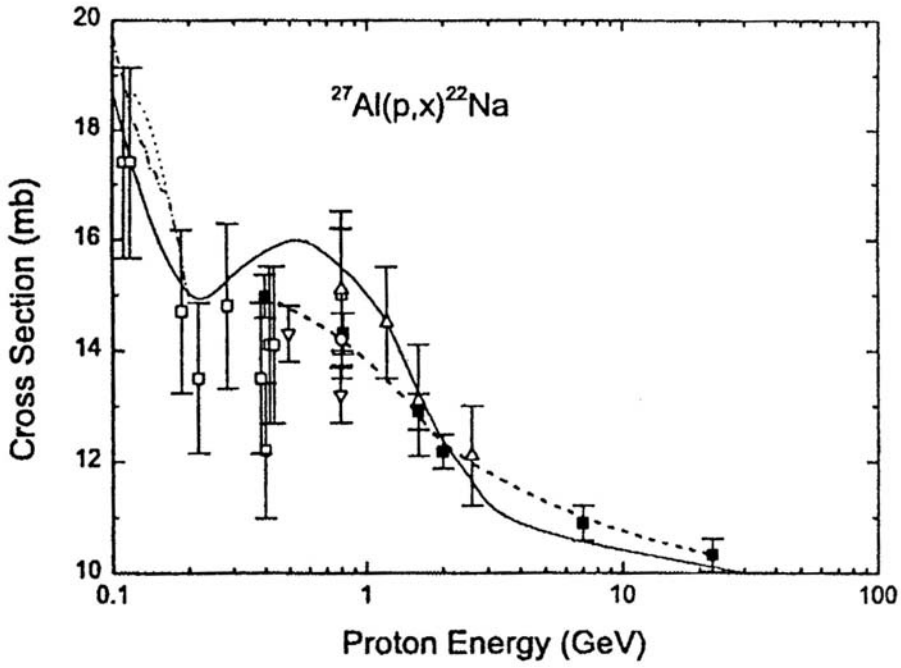

Fig. 5 – Cross–section for the production of the ^{22}Na via the p+^{27}Al reaction as a function of the incident proton beam energy [31].

Four different irradiations were performed with the enriched $^{179}HfO_2$ targets at proton energies of 255, 155, 130 and 110 MeV, respectively. The corresponding mean energies taking into account the energy loss in the targets are 242, 139, 112 and 90 MeV, respectively. We estimate that the accuracy of these values is within ±5 MeV. These effective energy

values will be used for the further analysis and interpretation of the experimental data. Since the thickness of the targets is relatively small, the measured yield of the product nuclei can be considered proportional to the mean cross–section because secondary reactions effects are negligible. The irradiation of the Al holders together with the target material provides a very reliable calibration method of the measured cross–sections. Absolute cross–section values were determined by comparison to the measured yield of ^{22}Na produced in the reaction (p+Al). The cross–sections for the production of ^{22}Na were accurately measured as a function of the incident proton beam energy [31]. The excitation function taken from Ref. [31] is shown in Fig. 5.

The use of enriched Hafnium in oxide form eliminated the presence of Zr in the samples due to the mass and chemical separation processes. As discussed in [33] the samples made of metallic natural Hafnium contained a relatively large amount of Zirconium and its spallation produced many background radioactive nuclides that introduced large uncertainties in the evaluation of fission fragment yields from the (p+^{nat}Hf) reaction. In the present case, the spallation of the large amount of Al contained in the targets produces long–lived radioactive nuclides that create a high γ–ray background over a wide range of γ–ray energies: E_γ=1274.6 and 511 keV in ^{22}Na, and E_γ=477.6 keV in ^{7}Be. The decay patterns of ^{7}Be and ^{22}Na radionuclides are schematically shown in Fig. 6. The 511 keV γ–ray line correspond to the positron annihilation peak. A large Compton continuum is present at γ–ray energies $E_\gamma \leq$ 1274.5 keV and makes difficult the measurement of the low intensity γ–ray lines from some fission fragments and isomers.

The ^{7}Be and ^{22}Na radionuclides are also produced in the (p+^{179}Hf) reaction but with a cross–section much lower than in the (p+Al) reaction.

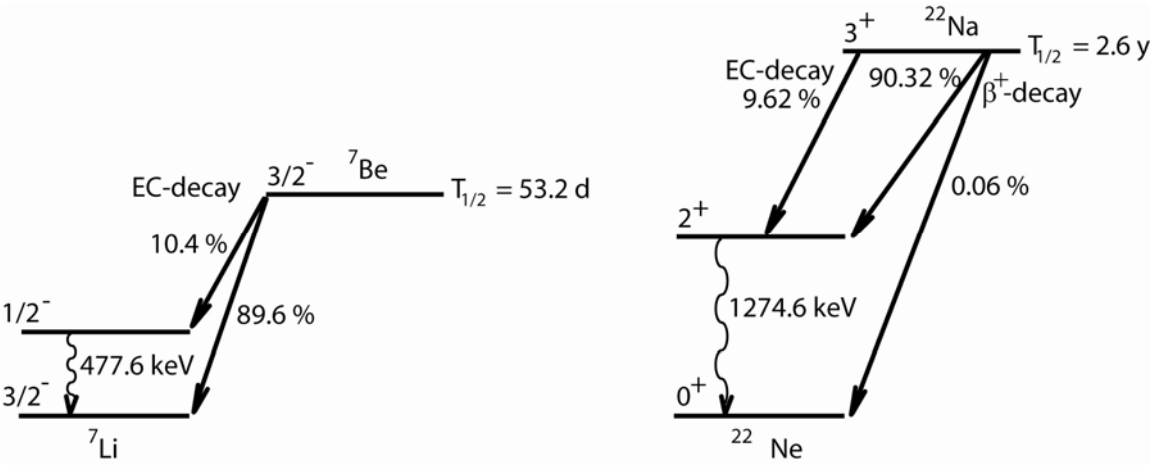

Fig. 6 – Decay schemes of the ^{7}Be and ^{22}Ne radionuclides produced in the (p + ^{27}Al) reaction. The information is taken from Ref. [34]. The annihilation of the positron emitted following the β^+–decay of ^{22}Na leads to the 511 keV peak in the γ–ray spectra.

Gamma–ray activity spectra were recorded 5 times during a period of 6 months following the irradiation of the four enriched $^{179}HfO_2$ targets. The measurements were performed with a

standard Canberra 20% coaxial HP Ge detector and a planar X-ray spectrometer. The signals from the detectors were processed by a high–rate spectroscopy amplifier (ORTEC 973) and a multichannel buffer (ORTEC 921). This spectroscopic chain can sustain counting rates up to 20 kcounts/s without significant deterioration of the γ–ray energy resolution. Since each sample had a different γ–ray background, both as intensity and composition, for each measurement we had to optimize the sample – detector distance and the absorbers (Pb, Cd and Cu) in front of the detectors to maintain the counting rate of the detectors below the 20 kcounts/s limit. The γ–ray spectra were recorded with the MAESTRO program delivered with the ORTEC multichannel buffer and saved on disk for analysis. The spectra for the 20% HP Ge detector were recorded on 8192 channels with an energy spread of about 0.43 keV/channel while the spectra from the planar detector were recorded on 4096 channels with an energy spread of about 0.17 keV/channel. The absolute yields of the radionuclides were estimated from the analysis of the γ–ray spectra and by using the standard equations for radioactive decay and accumulation. The decay properties of the radionuclides were taken from [34]. Identification of the γ–ray lines and the measurement of their intensity were done with the software package DEIMOS [35]. A fit of the γ–ray lines is performed and the half-width, energy, area and standard deviation were measured with accuracy determined by the statistics accumulated in the lines and the quality of the fitting procedure.

The detection efficiency was measured separately for each sample – detector distance and absorber thickness with standard γ–ray calibration sources. Well known intense γ–ray lines emitted by the samples themselves were also used for efficiency calibration; they have the advantage of taking into account the self–absorption of the γ rays in the target material.

The first measurement of the γ–ray activity of the samples was performed after about two weeks of cooling time. This limits the identification of the produced radionuclides to those with lifetimes longer than about 2 days. The measurements were repeated one month and 2.5 months after the irradiation. Since the background activity was still too high to allow identification of the weak activity associated with the decay of the ^{178m2}Hf isomer we performed the chemical separation of the Hf fraction from the samples. The chemical treatment in this case was different from the previous investigated systems since it had to provide purification of the bulk Hf material from all radioactive micro–admixtures (for the previous cases we developed a chemical method to isolate the Hf fraction from the bulk material – Ta, W, Re). A large effort was dedicated to eliminate the huge γ–ray activity associated to the decay of ^{22}Na; after several purification cycles the level of this activity was reduced such to allow a reliable measurement of the ^{178m2}Hf yield. After the chemical purification of the irradiated material two other measurements of the activity were performed.

5. Results and discussion

In Fig. 7 we show the spectra corresponding to the irradiation of the samples at three different proton energies after a cooling time of about three weeks. The samples were not yet chemically processed.

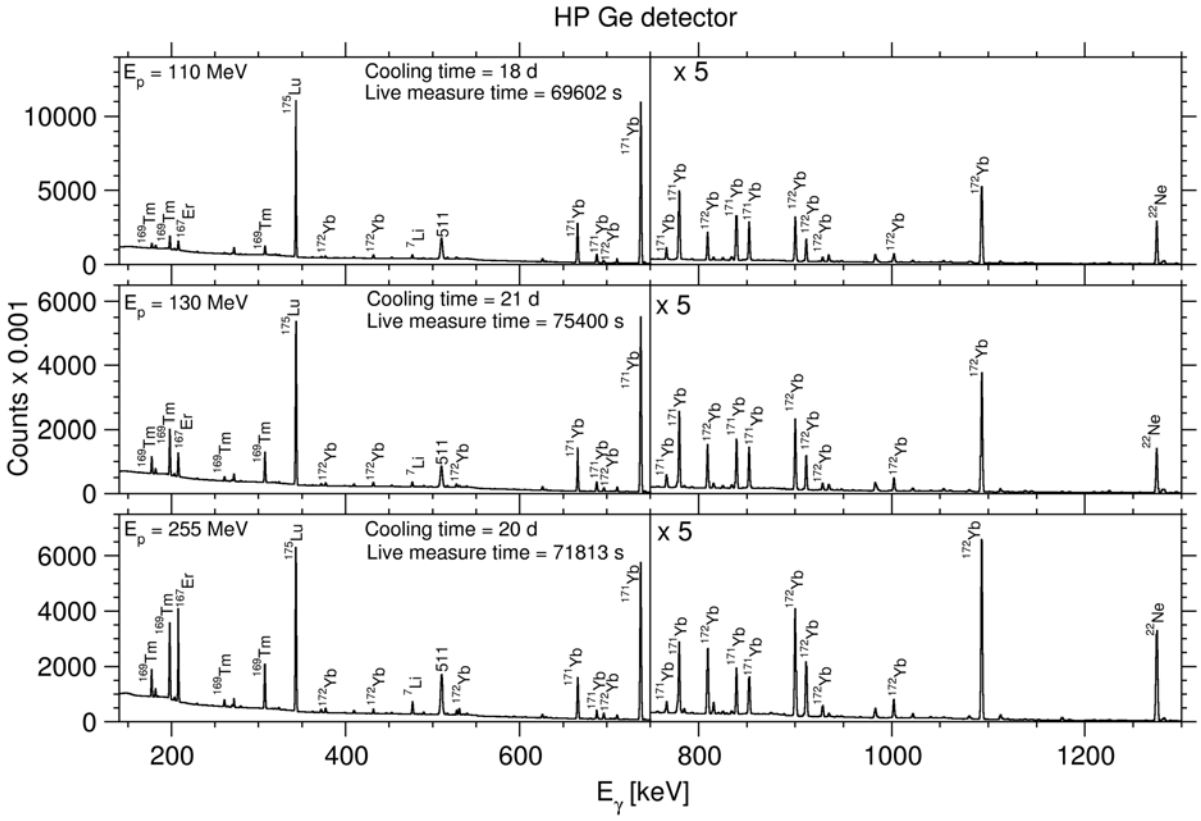

Fig. 7 – Gamma–ray activity spectra recorded with the 20% HPGe detector from three samples irradiated with protons of 110, 130 and 255 MeV, respectively. The measurements were performed after a short cooling time and before chemical purification of the samples was performed. The cooling time of the samples (in days) and the live measure time, i.e. corrected for the dead time of the acquisition system, (in seconds) are specified on the figure. Gamma–rays are labeled with the radionuclide to which they belong. The 511 keV γ–ray line is the positron annihilation peak and correspond to β^+–decay processes.

The strongest γ–ray lines in the spectra correspond to the following production – decay chains (the most intense γ–ray lines connected to each decay chain are specified with their relative intensities):

$^{179}\mathrm{Hf}(\mathrm{p,p'12n})^{167}\mathrm{Hf} \xrightarrow{EC(2.05\,\mathrm{m})} {}^{167}\mathrm{Lu} \xrightarrow{EC(51.5\,\mathrm{m})} {}^{167}\mathrm{Yb} \xrightarrow{EC(17.5\,\mathrm{m})} {}^{167}\mathrm{Tm} \xrightarrow{EC(9.25\,\mathrm{d})} {}^{167}\mathrm{Er}$

γ–rays in ^{167}Er: 207.8 keV;

$^{179}\mathrm{Hf}(\mathrm{p,p'10n})^{169}\mathrm{Hf} \xrightarrow{EC(3.24\,\mathrm{m})} {}^{169}\mathrm{Lu} \xrightarrow{EC(34.06\,\mathrm{h})} {}^{169}\mathrm{Yb} \xrightarrow{EC(32.03\,\mathrm{d})} {}^{169}\mathrm{Tm}$

γ–rays in ^{169}Tm: 109.8, 130.5, 177.2, 198.0 and 307.7 keV with relative intensities: 17, 11, 22, 35 and 10, respectively;

$^{179}\mathrm{Hf}(\mathrm{p,p'\ 8n})^{171}\mathrm{Hf} \xrightarrow{EC(12.1\,\mathrm{h})} {}^{171}\mathrm{Lu} \xrightarrow{EC(8.24\,\mathrm{d})} {}^{171}\mathrm{Yb}$

γ–rays in ^{171}Yb: 667.4, 689.3, 712.6, 739.8, 780.7, 839.9 and 853.1 keV with relative intensities: 11, 2, 1, 48, 4, 3 and 3, respectively;

$^{179}\mathrm{Hf}\,(\mathrm{p,p'\ 7n})^{172}\mathrm{Hf} \xrightarrow{EC(1.87\,\mathrm{y})} {}^{172}\mathrm{Lu} \xrightarrow{EC(6.7\,\mathrm{d})} {}^{172}\mathrm{Yb}$

γ–rays in ^{172}Lu: 122.9 (1), 125.8 (11) and 127.9 (2) keV with relative intensities: 1, 11 and 2 respectively;

γ–rays in ^{172}Yb: 112.8, 181.5, 279.7, 377.5, 490.4, 1002.8 and 1093.7 keV with relative intensities: 1, 21, 1, 3, 2, 5 and 63, respectively;

$^{179}\mathrm{Hf}\,(\mathrm{p,p'\ 4n})^{175}\mathrm{Hf} \xrightarrow{EC(70\,\mathrm{d})} {}^{175}\mathrm{Lu}$

γ–rays in ^{175}Lu: 343.4 and 433 with relative intensities: 80 and 1, respectively;

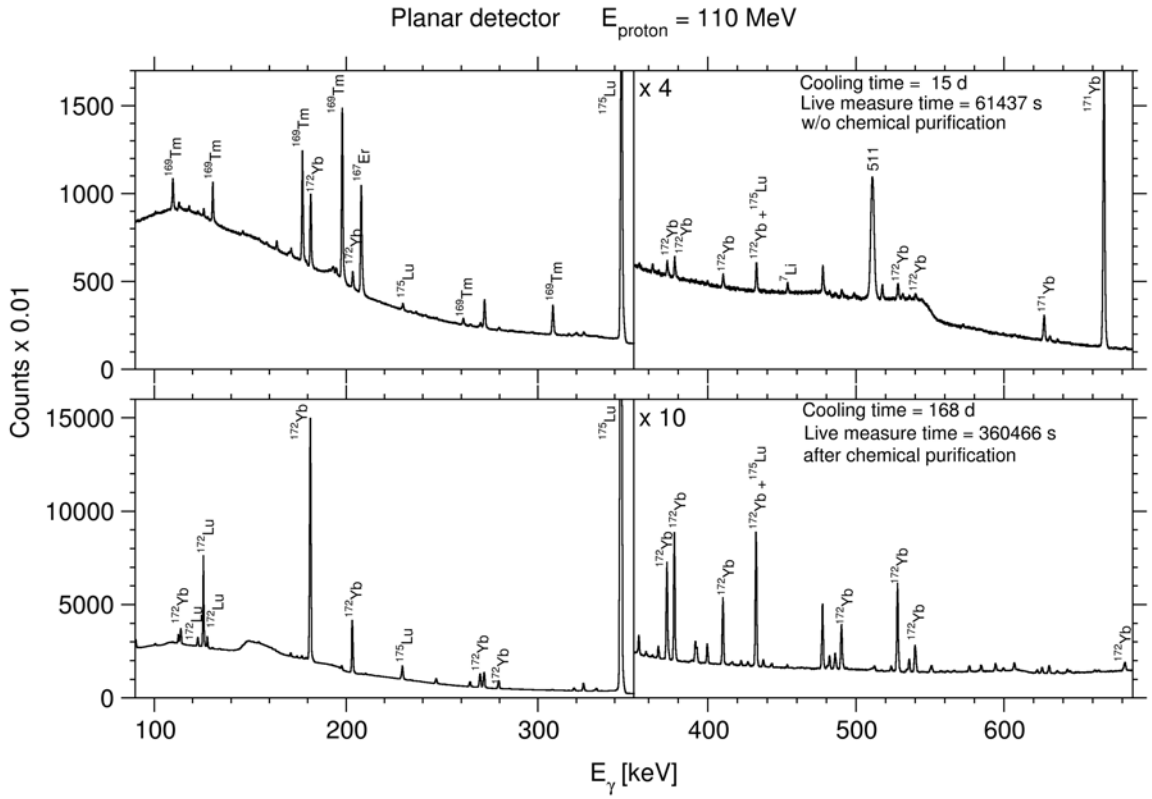

Fig. 8 – Gamma–ray activity spectra measured with the planar detector from the sample irradiated with protons of 110 MeV at two different time moments; the upper spectrum was recorded at short time after the irradiation while the lower spectrum was taken almost six months after the irradiation and after chemically processing of the sample.

We notice that at higher energies the radionuclides populated through emission of many particles (e.g., ^{169}Tm) are favored relatively to the ones populated with less particles emission (e.g., ^{175}Lu). We also observe that at the highest proton energy the production of ^{7}Be and ^{22}Na in the Al backing is substantially increased.

In Fig. 8 we compare two γ–ray spectra recorded with the planar detector from the sample irradiated with protons of 110 MeV. The upper spectrum was recorded at short time after the irradiation. The lower spectrum was recorded 168 days after the irradiation and after

the chemical purification of the sample. The decay–out of the short–lived isomers during the cooling time and the chemical processing of the samples efficiently removed many radionuclides from the sample and the γ rays related to their decay disappeared from the spectrum. We can notice the removal of ^{169}Tm and ^{171}Yb as well as of the radionuclides produced through the irradiation of the Al backing. As a result a strong reduction of the Compton background is evident in the lower spectrum. The lower activity produced a lower counting rate in the Ge detector and the resolution of the recorded γ–ray peaks improved noticeably. The better quality spectra allowed for the lowering of the observational limit enough to measure accurately the activity following the decay–out of the ^{178m2}Hf isomer.

We notice that the dominant radioactive contaminants of the samples that still survive after cooling for long a time and chemical purification are ^{172}Hf and ^{175}Hf. Both of these radionuclides are long–lived and cannot be eliminated through chemical purification.

The number of atoms of a given species of nuclei and their relative yields are determined from the measured area of the γ–ray lines. The absolute calibration of the yields is done by comparison with the yield of ^{22}Na.

The yield, Y, of a reaction product per one bombarding proton, is defined as:

$$Y = \int_{E_{min}}^{E_{max}} \sigma(E) \left(\frac{dE}{dx} \right)^{-1} dE \,, \qquad (1)$$

were E_{max} and E_{min} define the proton energy range in a target of known thickness, σ(E) is the cross–section, and dE/dx is the energy dependent stopping power of protons in the target material expressed in MeV/at·cm^{-2} if E is in MeV and σ in cm^2. The mean cross–section is connected with the yield through the expression:

$$\overline{\sigma} = Y \left[\int_{E_{min}}^{E_{max}} \left(\frac{dE}{dx} \right)^{-1} dE \right]^{-1} . \qquad (2)$$

Production cross–sections for many radioactive nuclei were determined. The measured values are reported in Tables 2 and 3. The errors reported in the tables are only statistical errors; systematic errors due to the absolute calibration of the cross–section values and the incomplete accumulation of the yield in isobaric decay chains are not included. The energy of the most intense γ rays used to estimate the production yields are reported in Table 2 together with the lifetime of the radioactive nuclei.

Table 2. Cross–section values (in mbarn) for the spallation products with the ^{nat}Hf and ^{179}Hf targets measured at mean proton energies of 235 and 242 MeV, respectively. Errors are given in brackets. The energy of the most intense γ rays used for estimating the cross–section values are specified in the table. The lifetime of the radionuclides is also reported.

Isotope	$T_{1/2}$	E_γ [keV]	Type of yield	^{nat}Hf + p @235 MeV	^{179}Hf + p @242 MeV
^{179m2}Hf	25.1 d	453.7; 362.3	Indep.	0.33(6)	0.44(3)

^{178m2}Hf	31 y	574.2; 495.0	Indep.	0.15(3)	0.39(6)
^{175}Hf	70 d	343.4; 432.8	EC-cum.	80(3)	76(3)
^{172}Hf	1.87 y	1093.6; 900.7	EC-cum.	69(3)	75(3)
^{177g}Lu	6.65 d	249.7	Indep.	–	25(4)
^{177m}Lu	160.4 d	413.7; 418.5	Indep.	0.49(6)	0.90(9)
^{174g}Lu	3.31 y	1241.8	Indep.	13.2(15)	13.06)
^{174m}Lu	142 d	992.1	Indep.	7.4(15)	9.9(15)
^{173}Lu	1.37 y	272.0	EC-cum.	115(7)	111(4)
^{172}Lu	6.7 d	1093.6; 900.7	Indep.	24(3)	27.9(6)
^{171}Lu	8.22 d	739.8; 667.4	EC-cum.	124(8)	122(5)
^{170}Lu	2 d	985.1	EC-cum	–	128(13)
^{169}Yb	32.0 d	307.7	EC-cum.	98(7)	91(3)
^{166}Yb	2.36 d	2052.4	EC-cum.	90(15)	48(6)
^{168}Tm	93.1 d	447.5; 720.3	Indep.	1.5(2)	2.3(3)
^{167}Tm	9.25 d	207.8	EC-cum.	101(7)	88(5)
^{160}Tb	72.3 d	1177.9	Indep.	0.015(3)	0.024(6)
^{156}Tb	5.35 d	534.3	Indep.	3.4(2)	0.20(5)
^{155}Tb	5.32 d	367.4	EC-cum.	20(8)	3.0(6)
^{149}Gd	9.3 d	748.2	EC-cum.	1.0(7)	0.09(3)
^{146}Gd→^{146}Eu	48.3→4.5 d	633.7	EC-cum.	0.15(5)	0.021(5)
^{156}Eu	15.2 d	2097.7	β^--cum.	0.20(5)	-
^{149}Eu	93 d	277.0	EC-cum.	1.05(7)	-
^{148}Eu	54.5 d	550.3	Indep.	0.030(6)	-
^{110m}Ag	249.9 d	884.7	Indep.	0.025(8)	0.007(1)
^{106m}Ag	8.3 d	1045.8	Indep.	0.058(15)	0.041(15)
^{105}Ag	41.3 d	443.4; 644.5	EC-cum.	0.17(1)	0.108(31)
^{102m}Rh	207 d	475.1	Indep.	0.024(9)	0.010(3)
^{103}Ru	39.4 d	497.1	β^--cum.	0.026(12)	0.014(4)
^{95m}Tc	60 d	582.1	Indep.	0.035(10)	0.021(10)
^{95}Nb	34.97 d	765.7	Indep.	0.058(4)	0.081(9)
^{91m}Nb	60.9 d	1204.8	Indep.	0.21(4)	0.12(3)
^{95}Zr	64.0 d	756.7; 724.2	β^--cum.	0.048(3)	0.011(3)

^{88}Zr	83.4 d	392.9	β^+-cum.	1.16(12)	0.073(10)
^{88}Y	106.6 d	898.1; 1836.0	Indep.	0.53(6)	0.051(6)
^{87}Y	3.35 d	388.4	β^+-cum.	–	0.20(3)
^{85}Sr	64.8 d	514.0	β^+-cum.	1.14(12)	–
^{82}Sr	25.3 d	776.5	β^+-cum.	0.44(6)	0.056(6)
^{84}Rb	32.8 d	881.6	Indep.	0.16(2)	0.075(15)
^{83}Rb	86.2 d	520.4	β^+-cum.	0.95(7)	0.071(10)
^{75}Se	119.8 d	264.6	β^+-cum.	0.16(3)	–
^{72}Se	8.5 d	834.0	β^+-cum.	0.12(2)	0.10(1)
^{74}As	17.77 d	595.8	Indep.	0.14(3)	0.039(6)
^{65}Zn	244.3 d	1115.5	β^+-cum.	0.04(1)	0.026(4)
^{60}Co	5.27 y	1332.5	Indep.	0.016(5)	–
^{56}Co	78.8 d	2598.6	EC-cum.	0.006(1)	–
^{59}Fe	44.5 d	1291.6;1099.5	β^--cum.	0.028(6)	0.051(9)
^{54}Mn	312.2 d	835.9	Indep.	0.048(11)	0.017(5)
^{48}V	16 d	1312.1	EC-cum.	0.035(7)	–
^{22}Na	2.6 y	1274.5	β^+-cum.	0.023(4)	–
^{7}Be	53.3 d	477.8	Indep.	0.058(9)	–

Table 3. Cross–section values (in mbarn) for the spallation products with the ^{179}Hf targets measured at mean proton energies of 139, 112 and 90 MeV, respectively. Errors are given in brackets.

Isotope	^{179}Hf + p @ 139 MeV	^{179}Hf + p @ 112 MeV	^{179}Hf + p @ 90 MeV
^{179m2}Hf	0.50(4)	0.56(4)	0.79(4)
^{178m2}Hf	0.44(9)	0.62(10)	0.68(6)
^{175}Hf	98(3)	111(4)	153(5)
^{172}Hf	100(4)	115(4)	165(5)
^{177g}Lu	16(3)	12.5(25)	18(4)
^{177m}Lu	0.75(8)	0.73(10)	0.67(8)
^{174g}Lu	10.9(6)	11.6(6)	9.6(6)
^{174m}Lu	8.5(15)	7.8(16)	7.1(18)
^{173}Lu	133(4)	150(4)	200(5)
^{172}Lu	22.1(6)	17.6(6)	12.7(4)

^{171}Lu	147(5)	157(8)	210(7)
^{170}Lu	151(25)	178(31)	212(30)
^{169}Yb	90(4)	84(5)	35(2)
^{166}Yb	30(8)	16.3(25)	2.0(3)
^{168}Tm	0.88(11)	0.60(10)	0.31(5)
^{167}Tm	60(3)	26.3(15)	13(1)
^{160}Tb	0.019(6)	0.023(6)	–
^{156}Tb	0.09(3)	0.05(1)	–
^{155}Tb	0.36(6)	–	–
^{110m}Ag	0.012(4)	0.007(2)	0.018(4)
^{106m}Ag	0.060(15)	0.038(13)	0.027(11)
^{105}Ag	0.28(8)	0.16(5)	0.08(2)
^{102m}Rh	–	0.030(5)	0.021(5)
^{103}Ru	0.013(4)	0.011(3)	0.016(2)
^{95m}Tc	0.045(9)	0.028(5)	0.013(3)
^{95}Nb	0.058(6)	0.041(7)	0.044(8)
^{91m}Nb	0.09(3)	0.125(25)	0.11(3)
^{95}Zr	0.007(2)	0.009(3)	0.012(2)
^{88}Zr	0.076(14)	0.095(15)	0.134(15)
^{88}Y	0.036(12)	0.016(5)	0.025(8)
^{87}Y	0.014(3)	0.125(38)	0.17(3)
^{85}Sr	–	0.021(5)	–
^{82}Sr	0.088(19)	0.11(2)	0.104(25)
^{84}Rb	0.036(7)	0.018(4)	0.08(2)
^{83}Rb	0.04910)	0.053(8)	0.039(12)
^{72}Se	0.060(10)	0.061(13)	0.09(2)
^{74}As	0.028(6)	0.029(6)	0.028(9)
^{65}Zn	0.044(10)	0.023(6)	0.021(4)
^{59}Fe	0.036(6)	0.026(4)	0.032(3)
^{54}Mn	–	0.016(5)	0.011(4)

The mass dependence of the cross–section values is represented in Figs. 9 and 10 for the four different irradiations. The mean proton energies are reported on the figures. The figures show two distinct distributions: the largest one corresponding to the spallation products

peaked at mass numbers near the mass of the target material, and a smaller one located at masses A ≤ 110 corresponding to the fission fragments.

The spallation yield of a given mass A is determined by the cumulative yield of the end–point radionuclide in the corresponding isobaric chain decay. This nuclide accumulates normally the whole yield of the chain because the spallation products are typically neutron deficient and located far from the β–stability line. For the fission products, the mass yields are estimated with limited accuracy due to the incomplete accumulation of many products. This results in an additional scattering of the measured fission values distribution. The error bars shown in Figs. 9 and 10 include only the random errors. Even with these uncertainties, the fission peak is clearly identified in the mass distributions and allows for the estimation of the fission–to–spallation ratio with good enough accuracy. This is an important result as the available experimental information on the magnitude of this parameter and its dependence on the energy is scarce in the literature.

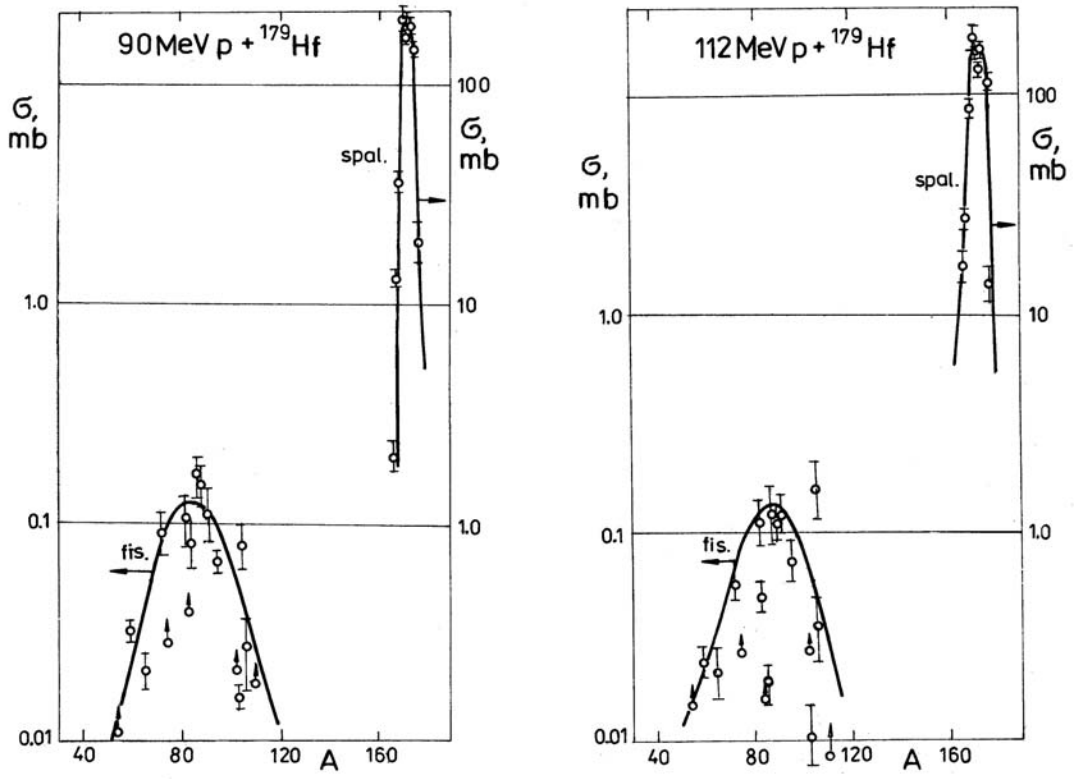

Fig. 9 – Cross–section values extracted from the irradiation of the enriched ^{179}Hf samples with protons of 110 (on the left panel) and 130 (on the right panel) MeV. The average proton energies are reported on the figures. Two different distributions are evident: the one close to the mass of the target material corresponds to the spallation products while the one at A ≤ 110 corresponds to the fission products.

The yields for the high–spin ^{179m2}Hf, ^{178m2}Hf and ^{177m}Lu isomers were successfully measured. The estimated absolute values are small because of the isomer–to–ground state ratio. These isomers can be populated only as independent yield and taking into account that they belong to isotopes with N/Z ratio far from the optimal values for the spallation process,

the resulting isomer–to–ground state ratios are very small. Since the ground states of these isotopes are stable we cannot measure their yields and the values reported in Tables 2 and 3 are only the independent yields for the isomers.

The γ–ray lines of ^{179m2}Hf and ^{177m}Lu were clearly observed even in the direct spectra but the activity of ^{178m2}Hf is much lower because of its long half–life and the γ–rays corresponding to its decay could be measured only after a long cooling time and chemical purification of the samples.

In Fig. 11 we show expanded regions of the spectra corresponding to the samples irradiated with 110 and 130 MeV incident protons after almost six months of cooling time and after chemical purification. The regions were selected around the energy corresponding to the gamma–ray decays $6^+ \rightarrow 4^+$ (325.5 keV), $8^+ \rightarrow 6^+$ (426.4 keV), and $11^- \rightarrow 9^-$ (495.0 keV) in ^{178}Hf populated by the decay of the ^{178m2}Hf isomer. It is clear that the reduction of the background is mandatory for an accurate analysis.

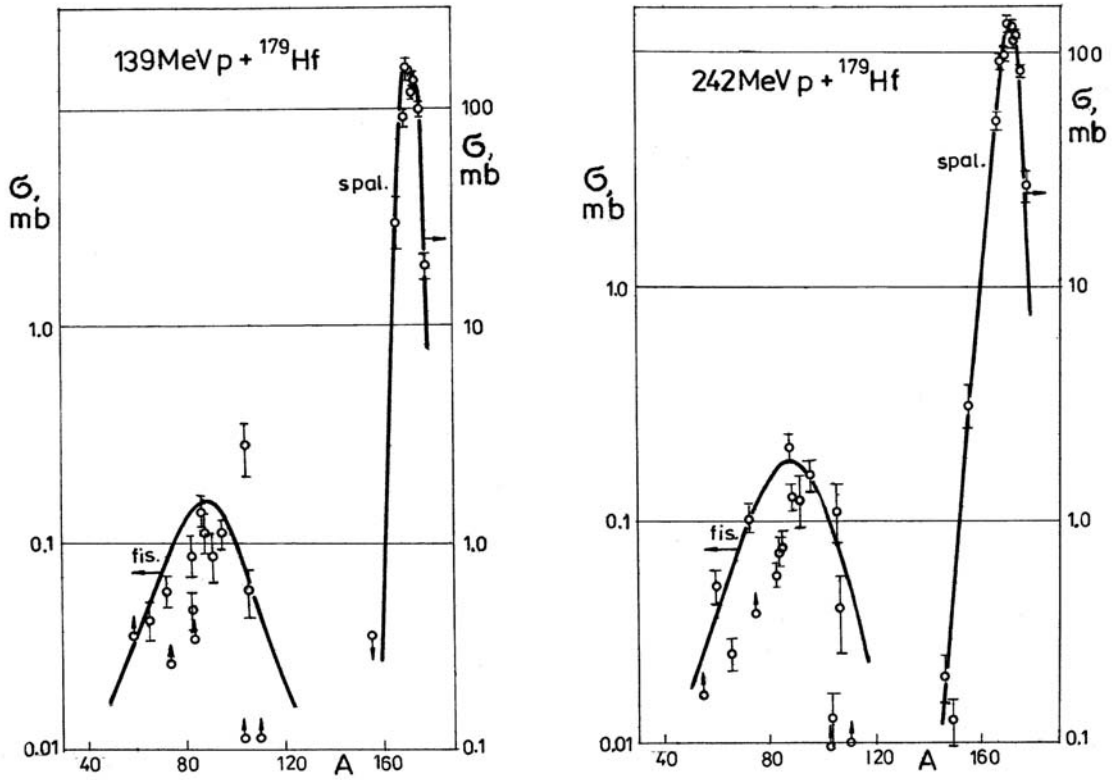

Fig. 10 – Cross–section values extracted from the irradiation of the enriched ^{179}Hf samples with protons of 155 (on the left panel) and 255 (on the right panel) MeV. The average proton energies are reported on the figures.

With the enriched ^{179}Hf target, the isomers of interest are produced exclusively through emission of only few nucleons. The ^{179m2}Hf isomer is populated via the ^{179}Hf(p,p′)^{179m2}Hf and the ^{178m2}Hf isomer through ^{179}Hf(p,p′n)^{178m2}Hf reaction. Emission of few nucleons (1 – 2) is a very special mode of the spallation process and its properties should significantly deviate from the case of many nucleons emission. Our previous studies concentrated mainly on the second type of spallation reactions where high energy proton beams favored population of the

isomers. Intuitively one can expect in the case of the Hf spallation a significant increase of the total cross–section at the lower energies close to 100 MeV since the final products are very close to the target nucleus. In the same time, one would expect a decrease of the isomer–to–ground state ratio as the lower beam energies would favor population of lower spin and excitation energy states. Currently it is impossible to make quantitative predictions for such enhancement or reduction as compared to the previous irradiations of the Ta, W and Re targets. The LAHET code simulations are not yet accurate enough for the case of only few nucleons emission. Thus, our discussion is based only on the measured cross–sections from the (p+Hf) reaction.

A summary of the measured cross–sections for the ^{179m2}Hf, ^{178m2}Hf and ^{177m}Lu isomers from the previous measurements at the highest beam energies is given in Table 4. The estimated isomer–to–ground state ratios are also reported in the table.

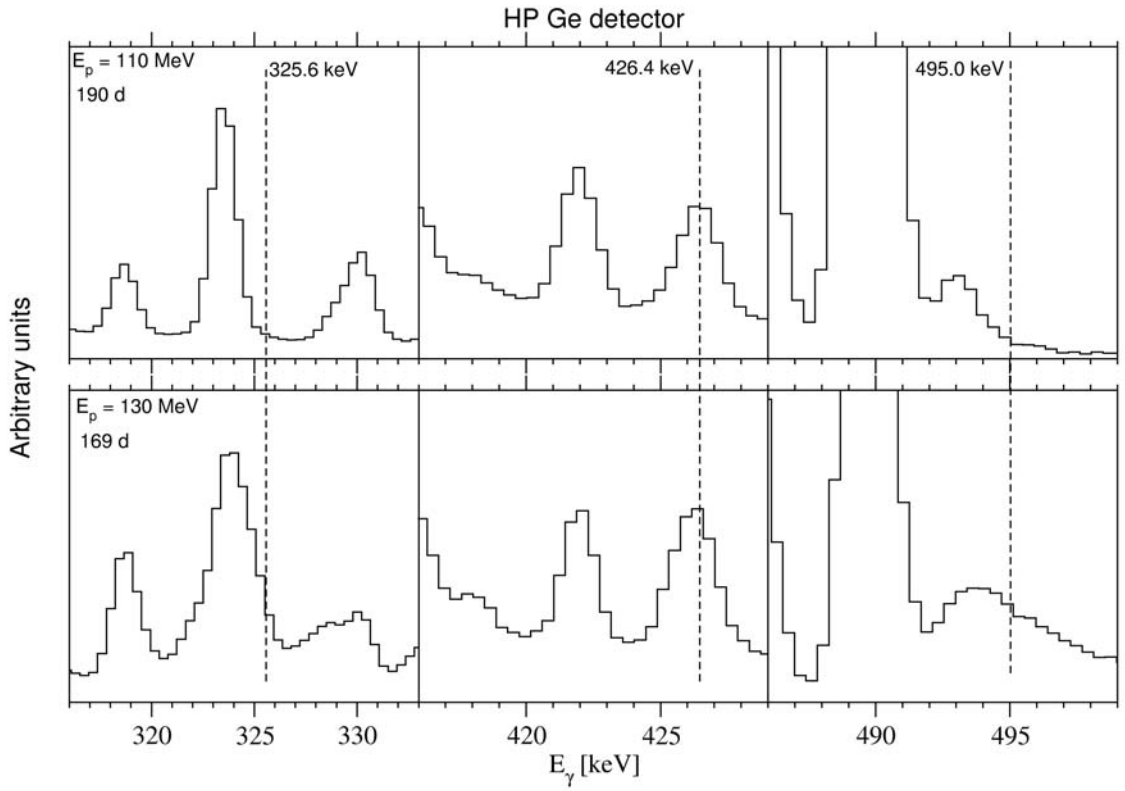

Fig. 11 – Selected regions of the γ–ray spectra recorded with the samples irradiated at 110 and 130 MeV after a long cooling time and chemical purification. The dotted lines indicate the position of the γ–ray lines populated by the decay of the ^{178m2}Hf isomer. The energy of the γ–ray transitions is indicated on the figure.

From Tables 2 and 3 we extracted the similar information for the case of the ^{179}Hf targets irradiations and we present it in Table 5.

According to the results reported in Tables 4 and 5 there is a significant increase for the production of the ^{177m}Lu isomer when ^{179}Hf targets are irradiated with lower energy protons. For ^{179m2}Hf we are at the same level as in the case when targets of ^{186}W were irradiated with

higher energy protons. As a general conclusion, we can assert that the irradiation of the Hf targets provide a higher production of the high–spin isomers ^{179m2}Hf, ^{177m}Lu and ^{178m2}Hf at proton energies near 100 MeV. An evident advantage of using Hf targets is the elimination of the ^{178}W production that contributed to the degradation of the isomer–to–ground state ratio in ^{178}Hf. The other main contaminants are produced at more or less the same level except for the lowest irradiation energy (100 MeV). If we compare the present results with the ones obtained from the irradiation of ^{nat}Hf samples [33] we notice the following facts:

- the yields of ^{177m}Lu and ^{179m2}Hf in the case of the ^{179}Hf irradiation are slightly higher; an enhancement factor of maximum 1.5 could be attained
- for the ^{178m2}Hf isomer the cross–section is by 2.5 times higher when ^{179}Hf is irradiated for all the proton energies, in good agreement with the qualitative discussion from Ref. [33] even if the absolute cross–section values are lower than the prediction.

Table 4. – Summary of the cross–sections and isomer–to–ground state ratios for the high–spin isomers of interest produced in the spallation reactions previously investigated. The values for the ground state population cross–section are calculated. The cross–sections for the main contaminants producing high gamma–ray background are given for comparison.

Nuclide	Reaction			
	p + ^{nat}Ta @ 660 MeV	p + ^{nat}W @ 650 MeV	p + ^{186}W @ 650 MeV	p + ^{nat}Re @ 660 MeV
Cross–section σ (mb)				
^{179}Hf^{m2}	0.52	0.36	0.80	0.12
^{178}H ^{m2}	0.31	0.18	0.48	0.13
^{177}Lu^{m}	0.15	0.13	0.26	0.04
^{178}W	5.90	23.00	21.80	36.00
^{175}Hf	56.00	55.00	55.60	59.00
^{172}Hf	47.00	53.50	57.40	55.00
^{173}Lu	61.00	61.00	60.00	61.00
Isomer–to–ground state ratio σ_m/σ_g				
^{179}Hf^{m2}	0.040	0.140	0.250	0.240
^{178}Hf^{m2}	0.021	0.044	0.092	0.140
^{177}Lu^{m}	0.103	0.210	0.290	0.400

The discussion on the possible enhancement of the ^{178m2}Hf production [33] was based on the simplistic assumption that the yield of ^{178m2}Hf is proportional to the ^{179}Hf isotope abundance in the target material. The experimental results do not confirm this assertion and help us understand the reaction mechanism behind the spallation processes with few nucleons emission. In Ref. [33] we concluded that the ^{178m2}Hf and ^{179m2}Hf isomers are produced mainly in the (p, p′n) reaction. If this would be the case, when irradiating the enriched ^{179}Hf samples one would expect a significant decrease of the ^{179m2}Hf isomer yield but the experimental data show a different behavior.

Table 5. – Summary of the cross–sections and isomer–to–ground state ratios for the high–spin isomers of interest produced in the spallation reactions with Hf targets. The cross–sections for the main contaminants producing high gamma–ray background are given for comparison.

Nuclide	Reaction			
	p + ^{179}Hf @ 110 MeV	p + ^{179}Hf @ 130 MeV	p + ^{179}Hf @ 155MeV	p + ^{179}Hf @ 255 MeV
	Cross–section σ (mb)			
^{179}Hf^{m2}	0.79	0.45	0.40	0.35
^{178}H ^{m2}	0.62	0.54	0.35	0.31
^{177}Lu^{m}	0.67	0.58	0.60	0.72
^{178}W	–	–	–	–
^{175}Hf	153	89	78	61
^{172}Hf	165	92	80	60
^{173}Lu	200	120	106	89

The values listed in Tables 2 and 3 demonstrate that the cross–section for the ^{179m2}Hf isomer is at the same level as in the case of irradiating ^{nat}Hf samples [33]. In the same time we notice that the ^{178m2}Hf isomer yield is only about 2.5 times larger than when irradiating ^{nat}Hf samples. These facts forced us to reconsider our previous very simple reasoning on the mechanisms leading to the population of the discussed high–spin isomers. The experimental results imply that besides the (p,p′n) reaction, assumed before as the only source of the high–spin isomers, also the (p,p′) and most probably the (p,p′2n) reactions contribute as well to the production of these isomers. In the light of the new experimental data, this is the only plausible explanation and we can conclude that the reaction channels with emission of 1, 2 and 3 nucleons are equally important for the population of the high–spin isomers ^{178m2}Hf and ^{179m2}Hf.

A strong dependence of the isomer yields on the spin difference ΔI of the initial and final states of the reaction (spin–deficit parameter) was discussed in Ref. [24] when the energies are of the order of MeV. In the case of spallation at energies E_p>100 MeV, the spin deficit parameter turns out to be relatively flat. All three isomers, ^{179m2}Hf (25/2 ħ), ^{178m2}Hf (16 ħ) and ^{177m}Lu (23/2 ħ) are characterized by similar cross–sections within a factor of two regardless of the variation of the final spin between 16 ħ and 9/2 ħ units. Such a flat behavior can be understood only by assuming a wide spin distribution of the spallation products. The width of distribution is probably as large as its mean value. We discussed qualitatively such a possibility when we investigated the spallation of the ^{nat}Ta with protons [29] and the present experimental results confirm our conclusions. It becomes evident that the models dealing with the spallation reaction mechanism have to include the angular momentum parameter as well because otherwise they will fail to correctly describe the population of the high–spin isomers and the isomer–to–ground state ratios.

6. Conclusions

We irradiated targets of enriched ^{179}Hf at four different proton energies, 110, 130, 155, and 255 MeV. After the irradiations the samples were left for cooling the activity due to the shorter lived radionuclides and eventually chemical purification of the samples was performed. This allowed us to determine the yields of many radioactive products through the activation method. The high-spin isomers ^{179m2}Hf, ^{178m2}Hf and ^{177m}Lu were identified and their cross–sections were measured.

Our measurements are a particular case of the spallation reactions. The high–spin isomers of interest result from channels with emission of one or two nucleons. Unfortunately, under these conditions the theoretical predictions of the reaction yield are not reliable and we could not estimate the isomer–to–ground state ratios. Our experimental results represent an important source of experimental data useful for the improvement of the theoretical models of the spallation processes.

The measured cross–section values show clearly that spallation with protons of $E_p \geq 100$ MeV the dependence of the isomer yield on the number of emitted nucleons and the spin of the target nuclei is relatively flat.

The use of enriched ^{179}Hf targets provides yields of the ^{178m2}Hf isomer that are by a factor about 2.5 higher than in the case of the ^{nat}Hf targets. The cross–sections measured with enriched ^{179}Hf targets are at the level of the ones measured with ^{186}W targets at high proton energies. The cross–section measured for ^{178m2}Hf at 130 MeV is similar to the cross–section measured with the 186W target at 660 MeV. The main advantage of using enriched ^{179}Hf targets is the low energy of the proton beam with benefits on the reduction of the irradiation costs and a lower level of the main radioactive contaminants and consequently, shorter cooling time of the samples before use.

An overview of the spallation reactions used for the production of the ^{178m2}Hf isomer was submitted to Romanian Reports in Physics in January 2008 and we prepare, currently, a paper to be submitted this year to Nuclear Instruments and Methods in Physics Research with the latest results presented in this report.

7. References

[1] K.N. CLAUSEN AND J. MESOT, *The route forward for Europe: The European Spallation Source (ESS)!*, Neutron News 18 (2007) 2;

[2] R.L. KUSTOM, *An overview of the spallation neutron source project*, Proceedings of the LINAC 2000 Conference, August 21–25, 2000, Monterey, California, USA; arXiv:physics/0008212v1;

[3] H. WATANABE, K. ASAHI, T. KISHIDA, H. UENO, W. SATO, A. YOSHIMI, Y. KOBAYASHI, D. KAMEDA, H. MIYOSHI, T. FUKUCHI, Y. WAKABAYASHI, T. SASAKI, M. KIBE, N. HOKOIWA, A. ODAHARA, B. CEDERWALL, K. LAGERGREN, ZS. PODOLYÁK, M. ISHIHARA AND Y. GONO, *Application of the high-spin isomer beams to the secondary fusion reaction and the measurement of g–factor*, Nuclear Physics A746 (2004) 540c;

[4] P.M. WALKER, *Isomer beams*, International Journal of Modern Physics E 15 (2006) 1637;

[5] U. KOSTER, R. CATHERALL, V.N. FEDOSEYEV, S. FRANCHOO, U. GEORG, M. HUYSE, K. KRUGLOV, J. LETTRY, V.I. MISHIN, M. OINONEN, H. RAVN, M.D. SELIVERSTOV, H. SIMON, P. VAN DUPPEN, J. VAN ROOSBROECK AND L. WEISSMAN, *Isomer separation and measurement of nuclear moments with the ISOLDE RILIS*, Hyperfine Interactions 127 (2000) 417;

[6] I. STEFANESCU, G. GEORGIEV, F. AMES, J. AYSTO, D.L. BALABANSKI, G. BOLLEN, P.A. BUTLER, J. CEDERKALL, N. CHAMPAULT, T. DAVINSON, A. DE MAESSCHALCK, P. DELAHAYE, J. EBERTH, D. FEDOROV, V.N. FEDOSSEEV, L.M. FRAILE, S. FRANCHOO, K. GLADNISHKI, D. HABS, K. HEYDE, M. HUYSE, O. IVANOV, J. IWANICKI, J. JOLIE, B. JONSON, TH. KROLL, R. KRUCKEN, O. KESTER, U. KOSTER, A. LAGOYANNIS, L. LILJEBY, G. LO BIANCO, B.A. MARSH, O. NIEDERMAIER, T. NILSSON, M. OINONEN, G. PASCOVICI, P. REITER, A. SALTARELLI, H. SCHEIT, D. SCHWALM, T. SIEBER, N. SMIRNOVA, J. VAN DEWALLE, P. VAN DUPPEN, S. ZEMLYANOI, N. WARR, D. WEISSHAAR, AND F. WENANDER, Coulomb Excitation of ^{68,70}Cu: First Use of Postaccelerated Isomeric Beams, Physical Review Letters 98 (2007) 122701;

[7] C. SCHEIDENBERGER, K. BECKERT, P. BELLER, F. BOSCH, C. BRANDAU, D. BOUTIN, L. CHEN, B. FRANZKE, H. GEISSEL, R. KNÖBEL, C. KOZHUHAROV, J. KURCEWICZ, S.A. LITVINOV, YU.A. LITVINOV, M. MAZZOCCO, G. MÜNZENBERG, F. NOLDEN, W.R. PLAß, M. STECK, B. SUN, H. WEICK AND M. WINKLER, *Isobar separation at FRS–ESR – a development towards pure isomeric stored beams*, Hyperfine Interactions 173 (2006) 61;

[8] R.G. HELMER AND C.W. REICH, *Decay of an isomeric state in ^{178}Hf with K≥16,* Nuclear Physics A114 (1968) 649;

[9] F.W.N. DE BOER, P. F. A. GOUDSMIT, B. J. MEIJER, J. C. KAPTEYN, J. KONIJN AND R. KAMERMANS, *The four quasi-particle ^{178}Hf isomeric state, its excitation energy and multipolarities of deexciting transitions*, Nuclear Physics A263 (1976) 397;

[10] S. DEYLITZ, B.D. VALNION, K.EL ABIARY, J. DE BOER, A. GOLLWITZER, R. HERTENBERGER, G. GRAW, R. KULESSA, CH. BRIANCON, D. LE DU, R. MEUNIER, M. HUSSONNOIS, O. CONSTANTINESCU, S. FORTIER, J.B. KIM, L.H. ROSIER, G. ROTBARD, YU.TS. OGANESSIAN, S. A. KARAMIAN, H.J. WOLLERSHEIM, H. FOLGER, J. GERL, TH. HAPP AND C. HATEGAN, *Inelastic deuteron scattering from the high-spin isomer ^{178}Hf^{m2} (16^{+})*, Physical Review C 53 (1996) 1266;

[11] S.M. MULLINS, G. D. DRACOULIS, A. P. BYRNE, T. R. MCGORAM, S. BAYER, W. A. SEALE AND F. G. KONDEV, *Rotational band on the 31 yr 16^{+} isomer in ^{178}Hf*, Physics Letters B393 (1997) 279; Erratum Physics Letters B400 (1997) 401; ;

[12] M.B. SMITH, P. M. WALKER, G. C. BALL, J. J. CARROLL, P. E. GARRETT, G. HACKMAN, R. PROPRI, F. SARAZIN AND H. C. SCRAGGS, *γ rays emitted in the decay of 31-yr ^{178}Hf* ^{m2}, Physical Review C 68 (2003) 031302;

[13] A.B. HAYES, D. CLINE, C.Y. WU, H. AI, H. AMRO, C. BEAUSANG, R.F. CASTEN, J. GERL, A.A. HECHT, A. HEINZ, H. HUA, R. HUGHES, R.V.F. JANSSENS, C.J. LISTER, A.O. MACCHIAVELLI, D.A. MEYER, E.F. MOORE, P. NAPIORKOWSKI, R.C. PARDO, CH. SCHLEGEL, D. SEWERYNIAK, M.W. SIMON, J. SREBRNY, R. TENG, K. VETTER AND H.J. WOLLERSHEIM , *Spin dependence of K mixing, strong configuration mixing, and electromagnetic properties of ^{178}Hf*, Physical Review C 75 (2007) 034308;

[14] W. KUTSCHERA, I. AHMAD, W.J. CHILDS, R.V.F. JANSSENS AND R.C. PARDO, Proceedings of the First International Conference on Radioactive Beams, Berkeley, 1989, World Scientific, Singapore, p.345;

[15] C.B. COLLINS AND J.J. CARROLL, *Progress in pumping a gamma–ray laser*, Hyperfine Interactions 107 (1997) 3;

[16] C.B. COLLINS, C. D. EBERHARD, J. W. GLESENER, AND J. A. ANDERSON, *Depopulation of the isomeric state ^{180}Ta^{m} by the reaction ^{180}Ta^{m}(γ,γ$^{'}$)^{180}Ta*, Physical Review C 37 (1988) 2267;

[17] S.-C. WU AND H. NIU, *Nuclear Data Sheets for A = 180*, Nuclear Data Sheets 100 (2003) 483;

[18] C.B. COLLINS, J.J. CARROLL, T.W. SINOR, M.J. BYRD, D.G. RICHMOND, K.N. TAYLOR, M. HUBER, N. HUXEL, P.V. NEUMANN–COSEL, A. RICHTER, C. SPIELER AND W. ZIEGLER, *Resonant excitation of the reaction $^{180}Ta^{m}(\gamma,\gamma')^{180}Ta$,* Physical Review C 42 (1990) 1813;

[19] D. BELIC, C. ARLANDINI, J. BESSERER, J. DE BOER, J.J. CARROLL, J. ENDERS, T. HARTMANN, F. KÄPPELER, H. KAISER, U. KNEISSL, E. KOLBE, K. LANGANKE, M. LOEWE, H.J. MAIER, H. MASER, P. MOHR, P.VON NEUMANN–COSEL, A. NORD, H.H. PITZ, A. RICHTER, M. SCHUMANN, F.–K. THIELEMANN, S. VOLZ AND A. ZILGES, *Photo–induced depopulation of the $^{180}Ta^{m}$ isomer via low–lying intermediate states: Structure and astrophysical implications,* Physical Review C 65 (2002) 035801;

[20] C.B. COLLINS, F. DAVANLOO, A.C. RUSU, M.C. IOSIF, N.C. ZOITA, D.T. CAMASE, J. M. HICKS, S.A. KARAMIAN, C.A. UR, I.I. POPESCU, R. DUSSART, J.M. POUVESLE, V.I. KIRISCHUK, N.V. STRILCHUK, P. MCDANIEL AND C.E. CRIST, *γ emission from the 31–yr isomer of ^{178}Hf induced by x–ray irradiation,* Physical Review C 61 (2000) 054305;

[21] C.B. COLLINS, N.C. ZOITA, A.C. RUSU, M.C. IOSIF, D.T. CAMASE, F. DAVANLOO, S. EMURA, T. URUGA, R. DUSSART, J. M. POUVESLE, C.A. UR, I.I. POPESCU, V.I. KIRISCHUK, N.V. STRILCHUK AND F.J. AGEE, *Tunable synchrotron radiation used to induce γ-emission from the 31 year isomer of ^{178}Hf,* Europhysics Letters 57 (2002) 677;

[22] S.A. KARAMIAN, *Comparative Analysis of the $^{178m2}Hf$ Yield at Reactions with Different Projectiles,* Physics of Atomic Nuclei (Yadernaya Fizica) 68 (2005) 1765;

[23] YU.TS. OGANESSIAN, S.A. KARAMIAN, Y.P. GANGRSKI, B. GORSKI, B.N. MARKOV, Z. SZEGLOWSKI, CH. BRIANCON, D. LEDU, R. MEUNIER, M. HUSSONNOIS, O. CONSTANTINESCU AND M.I. SUBBOTIN, *Production, chemical and isotopic separations of the long–lived isomer $^{178}Hf^{m2}$ ($T_{1/2}$=31 years),* Journal of Physics G: Nuclear and Particle Physics 18 (1992) 393;

[24] S.A. KARAMIAN, J.J. CARROLL, J. ADAM, E.N. KULAGIN AND E.P. SHABALIN **,** *Production of long–lived hafnium isomers in reactor irradiations,* High Energy Density Physics 2 (2006) 48;

[25] M.B. CHADWICK AND P.G. YOUNG, *Calculations of the production cross–sections of high–spin isomeric states in Hafnium*, Nuclear Science and Engineering 108 (1991) 117;

[26] J. REIJONEN, T.P. LOU, B. TOLMACHOFF, K.N. LEUNG, *Compact neutron source development at LBNL,* July 25, 2001, paper LBNL-47265;

[27] H.A. O'BRIEN, *Utilization of an intense beam of 800 MeV protons to prepare radionuclides,* Nuclear Instruments and Methods in Physics Research B 40/41(1989) 1126;

[28] *Production of Radionuclides at Intermediate Energies,* H. SCHOPPER Ed., Springer, Berlin, 1993, subvolume C;

[29] S.A. KARAMIAN, J. ADAM, D.V. FILOSSOFOV, D. HENZLOVA, V. HENZL, V.G. KALINNIKOV, N.A. LEBEDEV, A.F. NOVGORODOV, C.B. COLLINS, I.I. POPESCU, C.A. UR, *Accumulation of the $^{178m2}Hf$ isomeric nuclei through spallation with intermediate–energy protons of Tantalum and Rhenium targets*, Nuclear Instruments and Methods in Physics Research A 489 (2002) 448;

[30] S.A. KARAMIAN, J. ADAM, P. CHALOUN, D.V. FILOSSOFOV, V. HENZL, D. HENZLOVA, V.G. KALINNIKOV, N.A. KOROLEV, N.A. LEBEDEV, A.F. NOVGORODOV, C.B. COLLINS, I.I. POPESCU, C.A. UR, *Yield of radionuclides and isomers produced in the fragmentation of ^{nat}W and ^{186}W (97%) targets with protons at 630, 420 and 270 MeV*, Nuclear Instruments and Methods in Physics Research A 527 (2004) 609;

[31] G.L. MORGAN, K.R. ALRICK, S. SAUNDERS, F.C. CVERNA, N.S.P. KING, F.E. MERRILL, L.S. WATERS, A.L. HANSON, G.A. GREENE, R.P. LILJESTRAND, R.T. THOMPSON, E.A. HENRY, *Total cross sections for the production of ^{22}Na and ^{24}Na in proton–induced reactions on ^{27}Al from 0.40 to 22.4 GeV*, Nuclear Instruments and Methods in Physics Research B 211 (2003) 297;

[32] C.L. RAO AND L. YAFFE**,** *Nuclear reactions induced in Tantalum by protons of energy up to 84 MeV,* Canadian Journal of Chemistry 41 (1963) 2516;

[33] Third Interim Report to the EOARD Grant FA8655-04-1-3046-P00001;
[34] Table of Isotopes. Edited by R.B.Firestone, V.S.Shirley, et al. Eighth Edition, Wiley, New York, 1996;
[35] J. Adam *et al.*, Measurement Techniques 44, 93 (2001) ;

Dr. Calin A. Ur

Principal Investigator

March 16th, 2008